Increased Open-Circuit Voltage of Organic Solar Cells by Reduced Donor-Acceptor Interface Area

Koen Vandewal,* Johannes Widmer, Thomas Heumueller, Christoph J. Brabec, Michael D. McGehee, Karl Leo, Moritz Riede, and Alberto Salleo*

The best organic photovoltaic devices using electron donor (D)-electron acceptor (A) blends as active layer have achieved nearly 100% internal quantum efficiency (IQE),[1–4] resulting in overall power conversion efficiencies (PCE) of 6%-10% for single junctions.[5,6] Further improvements in PCE are expected to be achieved by increasing the amount of photons absorbed by the active materials, thereby increasing the external quantum efficiency (EQE), or by increasing the operating voltage, under the constraint that efficient charge generation and transport properties are not lost. Both operating voltage and PCE are limited by the open-circuit voltage (V_{oc}) of the solar cell.[7] When Ohmic contacts are deployed, V_{oc} is related to the recombination dynamics of the free charge carriers[8,9] and has been found to strongly correlate with the energy of the interfacial electron-hole pair or charge transfer (CT) state E_{CT}.[10]

Up to now, most progress in increasing the V_{oc} of organic solar cells has been made by designing new materials with different frontier energy levels,[11,12] thereby increasing the energetic distance between the highest occupied molecular orbital (HOMO) of the donor and the lowest unoccupied molecular orbital (LUMO) of the acceptor, which roughly equals E_{CT}.[13,14] Additionally, E_{CT} has been shown to be sensitive to morphological changes introduced by film processing or annealing techniques. For instance, decreasing the degree of structural order of both D and A phases at the interface increases both E_{CT} and V_{oc}.[15–17] Increasing E_{CT} will however only benefit photovoltaic performance as long as E_{CT} is lower than the optical gap of the neat donor (E_{D*}) and acceptor material (E_{A*}). It has recently been shown that for an E_{D*}-E_{CT} offset as low as 0.1 eV, a reasonably high IQE (>85%) can still be obtained.[18] This indicates that relatively small E_{D*}-E_{CT} offsets do not necessarily need to hamper free charge carrier generation. On the other hand, the difference between E_{CT} and qV_{oc} is never significantly smaller than 0.55 eV (q is elementary charge).[10,19] As comparison, for inorganic solar cells where the bandgap is the equivalent of E_{CT}, the difference between the bandgap and qV_{oc} can be as small as ~0.3 eV.[20,21] Hence, the exploration of methods for minimizing the loss between E_{CT} and qV_{oc} in organic solar cells will be crucial for improving their device efficiency.

In order to reduce E_{CT} – qV_{oc}, the recombination of free charge carriers needs to be reduced.[9,22] A complete understanding of molecular, interfacial and morphological structure factors determining this rate is currently lacking. However, as the D-A interfacial area determines the probability that electron and hole meet, the interfacial area available for electron-hole encounter and recombination, is expected to play a role.[22] There is therefore an opportunity to increase V_{oc} beyond current limits by reducing the D-A interfacial area.

In this work we study the influence of interfacial area on the V_{oc} of small molecule donor:C_{60} organic solar cells. We accurately determine E_{CT} by sensitive measurements of EQE and electroluminescence (EL) emission spectra, probing the weak absorption and emission bands related to direct CT state excitation and recombination, at photon energies below the optical gap of both neat D and A material.[10,23] We further correlate the amplitude of the low energy CT absorption band in the EQE spectrum with the amount of ground state D-A complexes, proportional to the interfacial area. We ensure a large variation in interfacial area, by using a low concentration (1%vol to 10%vol) of donor molecules in a C_{60} acceptor matrix. Such devices were shown to have remarkably high EQEs, even though the relatively weakly absorbing C_{60} is the main absorber.[24] We show that when varying the donor concentration and consequently the interfacial area in the low donor regime, E_{CT} remains constant. V_{oc} however, can be increased substantially (80–150 meV), solely by a 10-fold decrease in interfacial area, under the condition that proper Ohmic contacts are used. Our findings provide the basis for a new design rule for organic solar cells with increased V_{oc}.

Figure 1(a) and (b) shows the EQE(E) spectra of devices comprising 50 nm C_{60} doped with a low concentration (1%, 5% and 10% in volume) of 1,1-bis-(4-bis(4-methyl-phenyl)-amino-phenyl)-cyclohexane (TAPC) or N,N,N′,N′-tetrakis(4-Methoxy-phenyl)benzidine (MeO-TPD) as electron donor, sandwiched

Dr. K. Vandewal, Prof. M. D. McGehee, Prof. A. Salleo
Department of materials science and engineering
Stanford University
Stanford, CA94305, USA
E-mail: koen.vandewal@iapp.de; asalleo@stanford.edu
Dr. K. Vandewal, Dr. J. Widmer, Prof. K. Leo, Dr. M. Riede
Institut für Angewandte Photophysik
Technische Universität Dresden
George-Bähr-Straße 1, 01069, Dresden, Germany
T. Heumueller, Prof. C. J. Brabec
Institute of Materials for Electronics and Energy Technology (I-MEET)
FAU Erlangen Nürnberg 91058, Erlangen, Germany
Prof. K. Leo
King Abdullah University of Science and Technology (KAUST)
Thuwal 23955–6900, Saudi Arabia
Dr. M. Riede
Clarendon Laboratory
Department of Physics
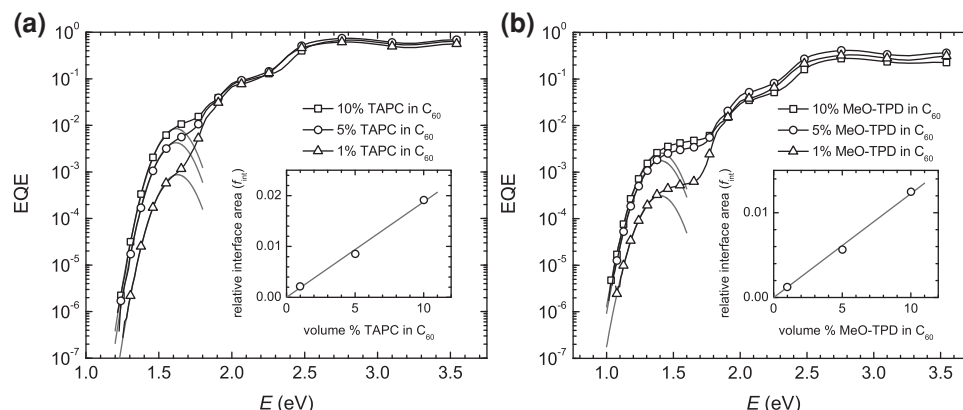University of Oxford
Oxford OX1 3PU, England, UK

Figure 1. EQE(*E*) spectra of low donor content active layers, sandwiched between ITO/MoO$_3$ and BPhen/Al contacts. Panel (a) shows EQE(*E*) spectra for photovoltaic devices with an active layer of 10%, 5% and 1% TAPC diluted in C$_{60}$. Panel (b) shows EQE(*E*) spectra for photovoltaic devices with an active layer of 10%, 5% and 1% MeO-TPD diluted in C$_{60}$. The CT absorption band is fitted with a Gaussian as described in the text and ref [10], yielding an E_{CT} of 1.45 eV for the TAPC:C$_{60}$ active layers and 1.20 eV for the MeO-TPD:C$_{60}$ active layers. The inset shows the relative amount of ground state donor-C$_{60}$ complexes as a function of donor content, determined as described in the text.

between Indium tin oxide (ITO)/MoO$_3$ (2 nm) and Bathophenanthroline (BPhen, 8 nm)/Al (100 nm) contacts. Even though C$_{60}$ is the main absorber in these low donor content devices, a relatively high maximum EQE (~60% at 450 nm, 2.7 eV for the 5% TAPC devices), as first reported by Tang et al.,[24] is obtained. The use of a sensitive EQE measurement setup allows us to present the spectra on a logarithmic scale, down to 10^{-6}, and resolve the optical transitions between 1.0 eV and 1.6 eV, below the optical gap of both C$_{60}$ (~1.6 eV), TAPC (~3.5 eV) and MeO-TPD (~3.1 eV). This sub-gap absorption feature is two orders of magnitude weaker than the main absorption and can be attributed to a weakly allowed electronic transition from the interfacial ground-state directly into the CT state.[25,26]

The CT absorption bands in the EQE spectra can be fitted with Gaussian curves, and are used to determine the energy of the CT state E_{CT}, via the procedure described in ref [10]. For all donor contents, the spectral shape of the CT band is found to be invariant and E_{CT} is determined to be 1.45±0.01 eV for TAPC:C$_{60}$ and 1.20 ± 0.01 eV for MeO-TPD:C$_{60}$. Such an independence of interfacial energetics is rather exceptional: When varying the D:A active layer morphology in solution processed or vacuum deposited (non-diluted) bulk heterojunction active layers by thermal annealing, or by varying the stoichiometry, E_{CT} has been shown to vary substantially (~0.2 eV).[15,16,27] Such shifts in E_{CT} have been attributed to changes in degree of aggregation or crystallization of either donor or acceptor component.[15,16,27] The use of a low donor content in a matrix of C$_{60}$ seems to prevent such changes in D-D or A-A intermolecular interactions, providing a unique system where the amplitude of the CT band, proportional to the density of ground state CT complexes, is varied over a wide range while keeping E_{CT} constant.

In order to quantify the relative interface area (f_{int}) for each device, the inset of Figure 1 shows the integrated signal of the CT band in the EQE spectrum, divided by the total integrated EQE. The linear relation of f_{int} with donor content, observed for both TAPC:C$_{60}$ and MeO-TPD:C$_{60}$ active layers, indicates that virtually every donor molecule is involved in D-A ground state CT complex formation implying that the donor molecules

are well dispersed in the C$_{60}$ matrix. By decreasing the donor content below 10%, the interfacial area is decreased linearly, without changing the interfacial energetics.

Photoluminescence (PL) and electroluminescence spectra of neat C$_{60}$ and TAPC:C$_{60}$ devices shown in **Figure 2**, confirm that at the investigated donor contents, down to 1%, the majority of the C$_{60}$ excitations are quenched (>90%) and form CT states. The PL spectra of the blend devices are dominated by CT emission, with a small but decreasing contribution of C$_{60}$ emission with increasing TAPC content. The electroluminescence (EL) spectra on the other hand, consist exclusively of CT emission. Moreover, the spectral position and shape of the EL CT
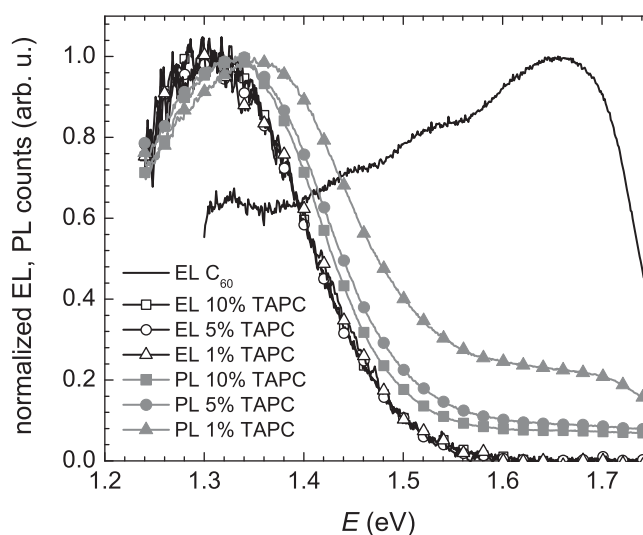

Figure 2. Normalized photoluminescence (PL) and electroluminescence (EL) spectra of the TAPC:C$_{60}$ devices. The EL spectrum of a pure C$_{60}$ device is shown as a reference. The excitation wavelength for the collection of PL spectra is 532 nm (2.3 eV), with the devices at open-circuit. For the measurement of EL spectra, an injection current of 10 mA.cm^{-2} was used. Both PL and EL spectra are dominated by CT emission between 1.2 eV and 1.5 eV.
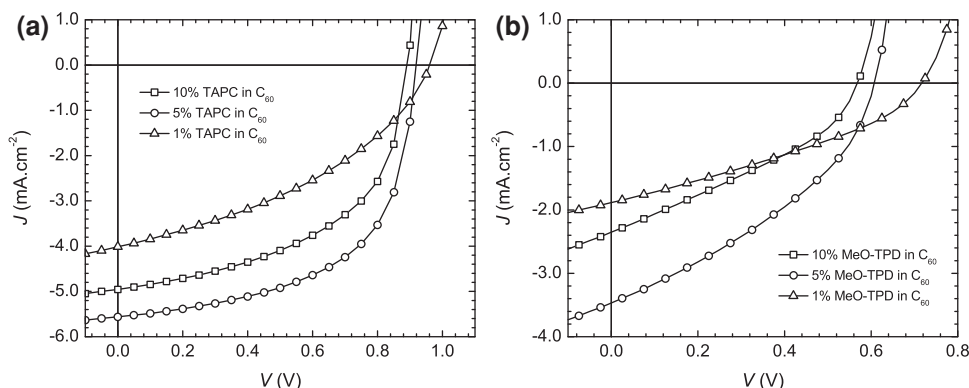
Figure 3. Current density – voltage (*JV*) curves under simulated solar illumination for devices comprising and active layer of (a) TAPC:C_{60} (b) MeO-TPD:C_{60} sandwiched between ITO/MoO$_3$ and BPhen/Al contacts. Optimal performance for these diluted cells is obtained for 5% of donor.

emission band does not vary with donor content, consistent with an invariant E_{CT} as observed in the EQE measurements.

Figure 3(a) and (b) show the current density-voltage (*JV*) curves of the photovoltaic devices, taken under 100 ± 2 mW.cm^{-2} mismatch corrected, simulated solar irradiation. The short-circuit current density J_{sc} (5.6 mA.cm^{-2}), fill factor (FF) (0.52) and PCE (3%) are largest for the 5% TAPC:C_{60} device, as previously demonstrated by Tang et al.[24] Even when the high (>3 eV) optical gap donor molecules are dispersed in such small amounts in a matrix of C_{60}, the solar cells perform remarkably well, and for the TAPC case, J_{sc} is mainly limited by the limited absorption of C_{60} in the visible and IR region. Most importantly, V_{oc} increases with decreasing donor content, even though the EQE and EL measurements clearly show that the effective gap E_{CT} does not vary with donor concentration.

In order to obtain more insights into V_{oc} and the related recombination dynamics, we perform photo-voltage decay measurements[28] on the TAPC:C_{60} devices. **Figure 4**(a) shows the lifetime τ of charge carriers, photo-generated by a small perturbation laser pulse as a function of V_{oc} set by a constant intensity bias light. For all concentrations, the carrier lifetime τ follows the relation

$$\tau = \tau_0 \exp\left(-\alpha V_{oc}\right) \qquad (1)$$

With α related to recombination order, ideality factor and temperature.[22,29] We find a value of $\alpha = 33$ V^{-1} for all TAPC concentrations, indicating that the recombination order and ideality factor are, in this case, independent on donor content. More importantly, as shown in Figure 4(b), τ_0 is inversely correlated to the interfacial area f_{int}. Indeed, less interfacial area will linearly decrease the probability for an electron in the C_{60} phase to meet a hole on TAPC, hereby increasing the carrier lifetime. This will result in an increased V_{oc}, since

$$V_{oc} = \frac{E_{CT}}{q} + n\frac{kT}{q}\ln\left(\frac{J_{sc}}{J_{00}}\right) \qquad (2)$$

with n the ideality factor, and J_{00} the dark saturation current. Values for J_{00} extracted from *JV* curves obtained in darkness (see supporting information) are plotted as a function of f_{int} in Figure 4(b). As predicted,[22,29] J_{00} is observed to be proportional to f_{int} and inversely proportional to τ_0. This results in the experimentally observed (Figure 3 and Figure 4(a)) logarithmic relation between V_{oc} and the interfacial area. Our results clearly show that carrier lifetime, dark saturation current and V_{oc} can be tuned independently of the interfacial energetics (E_{CT}).

Reducing the interfacial area available for recombination is therefore an effective way to reduce energy losses E_{CT}-qV_{oc}.
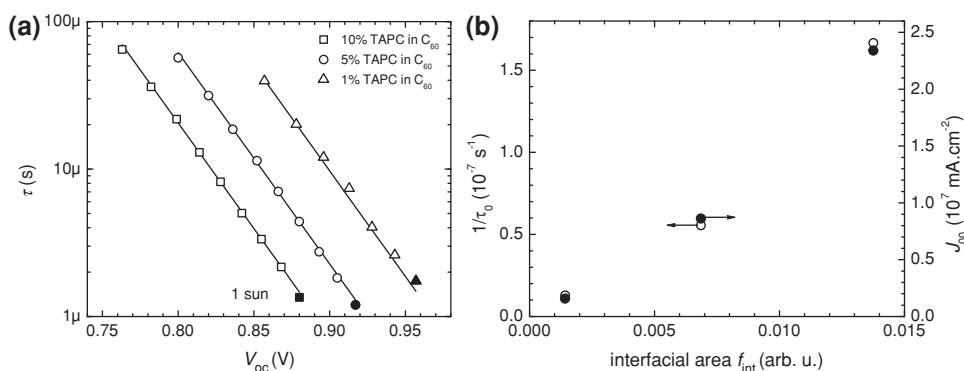

Figure 4. (a) Charge carrier lifetime τ as a function of bias voltage for 10%, 5% and 1% TAPC:C_{60} devices. The filled symbols represent data taken at a light intensity comparable to 1 sun solar intensity. The full lines are fits to the data using Equation (1), with $\alpha = 33$ V^{-1} and τ_0 dependent on TAPC content. (b) $1/\tau_0$ (left axis, open symbols) and J_{00} (right axis, closed symbols) as a function of interfacial area f_{int}, determined as described in the main text.

COMMUNICATION

Previously it has been found that under sunlight conditions, this loss is typically about 0.6 ± 0.05 eV.[10,15,30,31] In this work, we find for the optimal performing donor concentration (5%), $E_{CT}-qV_{oc}$ to be 0.52 eV for TAPC:C_{60} and 0.59 eV for MeO-TPD:C_{60} devices. This value decreases for 1% devices to 0.49 eV and 0.48 eV respectively.

Assuming radiative recombination as only recombination mechanism, an upper limit for V_{oc} can be calculated from the sensitively measured EQE spectra shown in Figure 1. Via the procedure described in refs [10,19,31] we perform these calculations for the TAPC:C_{60} devices, which all have an E_{CT} of 1.45 ± 0.01 eV. For the V_{oc} upper limit however, we find increasing values, from 1.21 V to 1.28 V, with the donor content decreasing from 10% to 1% (see supporting information). The difference between the experimentally obtained V_{oc} and upper limit is 0.32–0.33 V and depends logarithmically on the radiative fraction of the total recombination.[10,19,31] Since the experimentally obtained V_{oc} follows the same trend with donor content as predicted by the calculated upper limit, we conclude that for the TAPC:C_{60} devices, a reduction of the interfacial area decreases both the radiative and total recombination current, without affecting their ratio. Other pathways suggested to reduce the $E_{CT}-qV_{oc}$ difference, such a reduction of the electronic coupling between D and A, might affect only the radiative part of the recombination current, without affecting the dominating, non-radiative part. This will result in an increase of the upper limit for V_{oc}, but no change in measured V_{oc}.[30]

In conclusion, this work shows that V_{oc} can be tuned independently on interfacial energetics, and depends on the interfacial area available for charge carrier recombination. This implies that for D-A organic solar cells, an optimum interfacial area exists, sufficiently large to ensure exciton dissociation, but sufficiently small to allow a long charge carrier lifetime, beneficial for V_{oc}. Design of organic materials with larger exciton diffusion lengths will enable a reduced optimum interfacial area and thereby generate a smaller $E_{CT}-qV_{oc}$ difference, which must ultimately result in higher PCEs.

Experimental Section

Device Preparation: Thermally evaporated devices (base pressure $< 10^{-7}$ mbar) consist of glass/ITO (Thin Film Devices, USA) with 2 nm of MoO_3 as hole contact. Subsequently C_{60} (CreaPhys GmbH, Germany) is co-evaporated together with a low concentration (1%, 5% and 10% in volume) of 1,1-bis-(4-bis(4-methyl-phenyl)-amino-phenyl)-cyclohexane (TAPC) and N,N,N′,N′-tetrakis(4-Methoxy-phenyl)benzidine (MeO-TPD, Sensient GmbH, Germany) as electron donor. Finally, 8 nm of Bathophenanthroline (BPhen) capped with 100 nm of Al are evaporated as electron contact. The photovoltaic active area is defined as geometric overlap between ITO and Al contacts.

Sensitive EQE Measurements: Photovoltaic devices were illuminated by monochromated light of a 100 W quartz-tungsten-halogen lamp, modulated by an optical chopper at 280 Hz. The short-circuit current of the photovoltaic devices was measured at each photon energy using a lock-in amplifier and compared with the current obtained from a calibrated Ge or Si photodiode.

Electroluminescence and Photoluminescence Measurements: Spectra were measured using a spectrograph (ActonResearch SpectraPro 500i) equipped with a silicon CCD array detector (Hamamatsu), and were corrected for the instrument response and the conversion from wavelength to energy. The injection current used for electroluminescence was 10 mA.cm^{-2}. The excitation wavelength for photoluminescence was 532 nm.

Photovoltage Decay Measurements: Devices were illuminated using a white light LED with varying background light intensity, setting the DC V_{oc}. A pulsed 405 nm diode laser is used to excite the photovoltaic devices, causing a small voltage perturbation ΔV_{oc}. The laser intensity was adjusted to ensure $\Delta V_{oc} < 10$ mV $<< V_{oc}$, resulting in a single exponential decay. This photovoltage decay was recorded with an oscilloscope (1 MΩ input impedance) and reflects the carrier lifetime.[28]

[1] S. H. Park, A. Roy, S. Beaupré, S. Cho, N. Coates, J. S. Moon, D. Moses, M. Leclerc, K. Lee, A. J. Heeger, *Nat. Photonics* **2009**, *3*, 297.

[2] J. A. Bartelt, Z. M. Beiley, E. T. Hoke, W. R. Mateker, J. D. Douglas, B. A. Collins, J. R. Tumbleston, K. R. Graham, A. Amassian, H. Ade, J. M. J. Fréchet, M. F. Toney, M. D. McGehee, *Adv. Energy Mater.* **2013**, *3*, 364.

[3] Y. Liang, Z. Xu, J. Xia, S.-T. Tsai, Y. Wu, G. Li, C. Ray, L. Yu, *Adv. Mater.* **2010**, *22*, E135.

[4] S.-W. Chiu, L.-Y. Lin, H.-W. Lin, Y.-H. Chen, Z.-Y. Huang, Y.-T. Lin, F. Lin, Y.-H. Liu, K.-T. Wong, *Chem. Commun.* **2012**, *48*, 1857.

[5] J. You, L. Dou, K. Yoshimura, T. Kato, K. Ohya, T. Moriarty, K. Emery, C.-C. Chen, J. Gao, G. Li, Y. Yang, *Nat. Commun.* **2013**, *4*, 1446.

[6] G. Li, R. Zhu, Y. Yang, *Nat. Photonics* **2012**, *6*, 153.

[7] C. Deibel, V. Dyakonov, *Reports Prog. Phys.* **2010**, *73*, 096401.

[8] A. Maurano, R. Hamilton, C. G. Shuttle, A. M. Ballantyne, J. Nelson, B. O'Regan, W. Zhang, I. McCulloch, H. Azimi, M. Morana, C. J. Brabec, J. R. Durrant, *Adv. Mater.* **2010**, *22*, 4987.

[9] K. Vandewal, K. Tvingstedt, A. Gadisa, O. Inganäs, J. V. Manca, *Nat. Mater.* **2009**, *8*, 904.

[10] K. Vandewal, K. Tvingstedt, A. Gadisa, O. Inganäs, J. V. Manca, *Phys. Rev. B* **2010**, *81*, 125204.

[11] H.-Y. Chen, J. Hou, S. Zhang, Y. Liang, G. Yang, Y. Yang, L. Yu, Y. Wu, G. Li, *Nat. Photonics* **2009**, *3*, 649.

[12] S. Albrecht, S. Janietz, W. Schindler, J. Frisch, J. Kurpiers, J. Kniepert, S. Inal, P. Pingel, K. Fostiropoulos, N. Koch, D. Neher, *J. Am. Chem. Soc.* **2012**, *134*, 14932.

[13] M. C. Scharber, D. Mühlbacher, M. Koppe, P. Denk, C. Waldauf, A. J. Heeger, C. J. Brabec, *Adv. Mater.* **2006**, *18*, 789.

[14] J. Widmer, M. Tietze, K. Leo, M. Riede, *Adv. Funct. Mater.* **2013**, *23*, 5814.

[15] K. Vandewal, W. D. Oosterbaan, S. Bertho, V. Vrindts, A. Gadisa, L. Lutsen, D. Vanderzande, J. V. Manca, *Appl. Phys. Lett.* **2009**, *95*, 123303.

[16] F. Piersimoni, S. Chambon, K. Vandewal, R. Mens, T. Boonen, A. Gadisa, M. Izquierdo, S. Filippone, B. Ruttens, J. D'Haen, N. Martin, L. Lutsen, D. Vanderzande, P. Adriaensens, J. V. Manca, *J. Phys. Chem. C* **2011**, *115*, 10873.

[17] K. Vandewal, S. Himmelberger, A. Salleo, *Macromolecules* **2013**, *46*, 6379.

[18] K. Vandewal, Z. Ma, J. Bergqvist, Z. Tang, E. Wang, P. Henriksson, K. Tvingstedt, M. R. Andersson, F. Zhang, O. Inganäs, *Adv. Funct. Mater.* **2012**, *22*, 3480.

[19] K. Vandewal, K. Tvingstedt, O. Inganäs, in Semicond. Semimetals (Eds.: Uli Wüerfel, Michael Thorwart, Eicke R. Weber), Elsevier, **2011**, pp. 261–295.

[20] O. D. Miller, E. Yablonovitch, S. R. Kurtz, *IEEE J. Photovoltaics* **2012**, *2*, 303.

[21] M. A. Green, *Prog. Photovoltaics Res. Appl.* **2003**, *11*, 333.

[22] D. Credgington, J. R. Durrant, *J. Phys. Chem. Lett.* **2012**, *3*, 1465.

[23] K. Tvingstedt, K. Vandewal, A. Gadisa, F. Zhang, J. Manca, O. Inganäs, *J. Am. Chem. Soc.* **2009**, *131*, 11819.

[24] M. Zhang, H. Wang, H. Tian, Y. Geng, C. W. Tang, *Adv. Mater.* **2011**, *23*, 4960.

[25] K. Vandewal, A. Gadisa, W. D. Oosterbaan, S. Bertho, F. Banishoeib, I. Van Severen, L. Lutsen, T. J. Cleij, D. Vanderzande, J. V. Manca, *Adv. Funct. Mater.* **2008**, *18*, 2064.

[26] J. Lee, K. Vandewal, S. R. Yost, M. E. Bahlke, L. Goris, M. A. Baldo, J. V. Manca, T. V. Voorhis, *J. Am. Chem. Soc.* **2010**, *132*, 11878.

[27] M. L. Tietze, W. Tress, S. Pfützner, C. Schünemann, L. Burtone, M. Riede, K. Leo, K. Vandewal, S. Olthof, P. Schulz, A. Kahn, *Phys. Rev. B* **2013**, *88*, 085119.

[28] C. G. Shuttle, B. O'Regan, A. M. Ballantyne, J. Nelson, D. D. C. Bradley, J. de Mello, J. R. Durrant, *Appl. Phys. Lett.* **2008**, *92*, 093311.

[29] D. Credgington, R. Hamilton, P. Atienzar, J. Nelson, J. R. Durrant, *Adv. Funct. Mater.* **2011**, *21*, 2744.

[30] K. R. Graham, P. Erwin, D. Nordlund, K. Vandewal, R. Li, G. O. Ngongang Ndjawa, E. T. Hoke, A. Salleo, M. E. Thompson, M. D. McGehee, A. Amassian, *Adv. Mater.* **2013**, *25*, 6076.

[31] M. Gruber, J. Wagner, K. Klein, U. Hörmann, A. Opitz, M. Stutzmann, W. Brütting, *Adv. Energy Mater.* **2012**, *2*, 1100.